



**HAL**  
open science

# Design, implementation and characterization of an integrated current sensing in GaN HEMT device by using the current-mirroring technique

Van-Sang Nguyen, René Escoffier, Stephane Catellani, Murielle Fayolle-Lecocq, Jérémy Martin

## ► To cite this version:

Van-Sang Nguyen, René Escoffier, Stephane Catellani, Murielle Fayolle-Lecocq, Jérémy Martin. Design, implementation and characterization of an integrated current sensing in GaN HEMT device by using the current-mirroring technique. EPE'22 ECCE Europe - 2022 24th European Conference on Power Electronics and Applications, Sep 2022, Hanovre, Germany. pp.1-9. cea-04090553

**HAL Id: cea-04090553**

**<https://cea.hal.science/cea-04090553>**

Submitted on 5 May 2023

**HAL** is a multi-disciplinary open access archive for the deposit and dissemination of scientific research documents, whether they are published or not. The documents may come from teaching and research institutions in France or abroad, or from public or private research centers.

L'archive ouverte pluridisciplinaire **HAL**, est destinée au dépôt et à la diffusion de documents scientifiques de niveau recherche, publiés ou non, émanant des établissements d'enseignement et de recherche français ou étrangers, des laboratoires publics ou privés.

# **Design, implementation and characterization of an integrated current sensing in GaN HEMT device by using the current-mirroring technique**

Van-Sang NGUYEN, René ESCOFFIER, Stéphane CATELLANI, Murielle FAYOLLE-LECOCQ,  
Jérémy MARTIN

CEA - French Alternative Energies and Atomic Energy Commission  
50 avenue du Lac Léman  
Le Bourget du Lac - 73375, France  
Tel.: +33 / (0) 4 79 79 27 50  
E-Mail: van-sang.nguyen@cea.fr & rene.escoffier@cea.fr  
URL: www.cea.fr

## **Acknowledgements**

The Authors acknowledge CEA project “GaN4PV” for funding

## **Keywords**

«Current observer», «Current sensor», «Device characterization», «Double pulse test», «Dynamic  $R_{on}$ », «Fast fault detection», «Gallium Nitride (GaN)», «HEMT», «Measurement», «Over-current protection», «Power die», «Power integrated circuit», «Test bench», «Wide bandgap devices»,

## **Abstract**

Based on wide bandgap devices (WBG) characterization constraints, this work presents the design, implementation and characterization of an integrated current sensor in a GaN HEMT (Gallium Nitride High-Electron-Mobility Transistor) by using the current-mirroring technique. Two HEMTs are implemented in this design; the compromised between the size ratio of these two transistors in the current-mirroring circuit and the sensitivity of the sensor are taken into account on the device design phase. In the implementation phase, the auxiliary components are optimized for the operation of the sensor, and then the circuit with the integrated current sensing in GaN power device is characterized with a high temperature double pulse test method, up to 175°C.

## **Introduction**

Nowadays WBG semiconductors facilitate high efficient / compact energy conversion systems design [1-2]. Given their high switching speed, their dynamic characterization requires high bandwidth and low intrusive probes. Current measurement is made difficult by the intrusiveness of the probes, which modify the power switching loop impedance. In general, the measurement of switched currents can be performed by using a coaxial shunt, a current transformer or Rogowski-coil. However, these current sensors implementation introduce significant undesired parasitic inductance in the power loop of the device under test [3-4]. This article presents an integrated current sensor inside a monolithic GaN HEMT device allowing eliminating any intrusive current sensor. Thanks to its dynamic response, this current sensor can be employed with an integrated gate driver as a high-speed protection against short circuits responding within several tens nanoseconds. . The authors present a high temperature DPT (Double-Pulse-Tester) in which the sensitivity and the responses of the integrated current sensor in different temperatures is characterized. Thanks to an infrared beam, the device under test is heated up locally while all the auxiliary circuits are at room temperature.

## **Current sensing by integrating a current mirror**

The current-sense technique principle is based on current mirroring in integrated MOSFET at electronic circuits level [5]. A 100V-10A GaN HEMTs has been designed on a single die prototype as Fig. 1. In this prototype, the drains of the power and sensing devices are separated allowing to verify each device

independently. The work ongoing is dedicate to optimize the die's dimensions and implement additional functions by using the current sensor such as short-circuit protection in a new monolithic design.

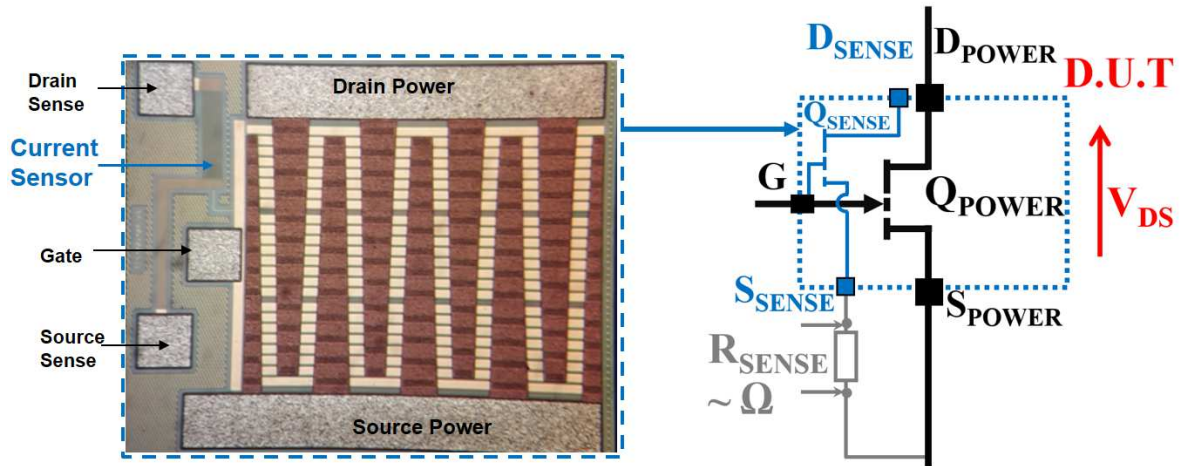


Fig. 1: GaN die (4.6mm x 4.3mm) with integrated current sensor and its schematic. Sense HEMT : 50x smaller Vs power HEMT

The gates of the power HEMT and the sense HEMTs share the same control signal. The current in the sense HEMT copies the current in the power HEMT with the ratio of the ON-state resistances and the value of the sense resistor as in equation (1).

$$\frac{I_{SENSE}}{I_{POWER}} = \frac{R_{DS\_ON\_POWER}}{R_{DS\_ON\_SENSE} + R_{SENSE}} \quad (1)$$

The ON-state resistance of the power HEMT equals several tens of  $m\Omega$ , the ON-state resistance of the sense HEMT is 50 times higher and the value of  $R_{SENSE}$  equals several  $\Omega$  in order to obtain a high sensitivity of the sensor. In addition, compared to the shunt-based approach [6], for which high temperature calibration can be tedious; the power/sense HEMTs share a similar thermal behavior and the selected  $R_{SENSE}$  has a very low tolerance (0.1%) corresponding to a temperature coefficient of resistance of 10 ppm/ $^{\circ}C$  for the high temperature operation.

A DFN (Dual-Flat No-leads) package is used for the implementation of the die; on which can be found three electrodes connected to the power drain and two electrodes to the power source. One electrode is connected to the drain sense and another to the source sense. As mention, a single control electrode is common to the two power/sense transistors. This packaged die is implemented in a DPT circuit Fig. 2.

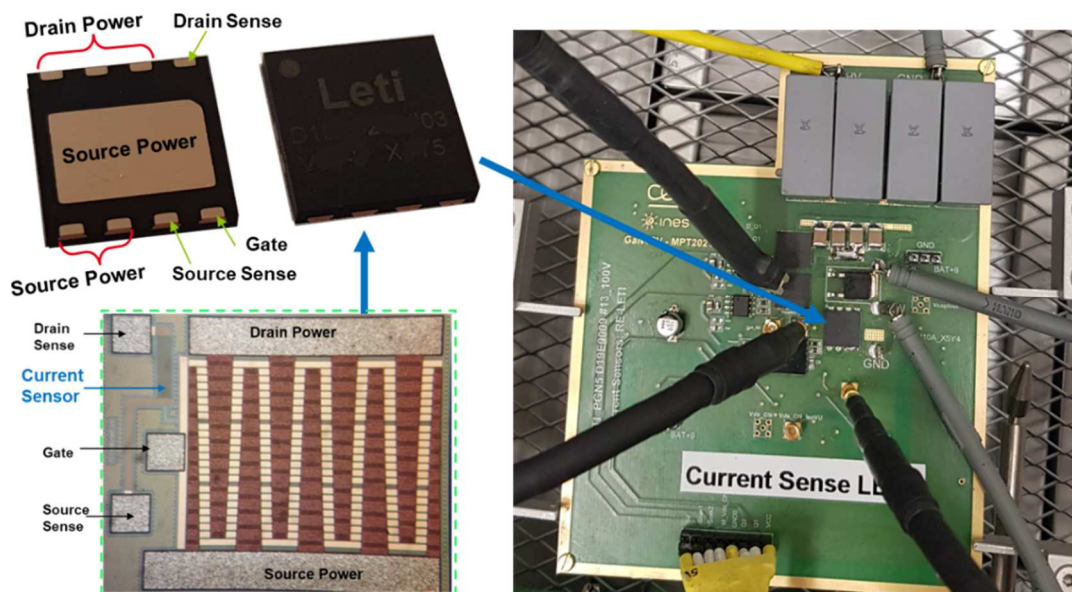


Fig. 2: GaN device with integrated current sensor in the characterization bench

The selected  $R_{SENSE}$  is very closely to the source sense pad and source power pad in order to avoid the parasitic inductance. Base on the current ratio in these two devices, the measurement of the voltage drop across  $R_{SENSE}$  is calibrated to demonstrate the current on the power device.

## The experimental results

As in a recent work on the high temperature dynamic characterization of GaN HEMT [7], the left side of Fig. 3 shows a high temperature test bench in which a specific profile of the infrared beam is applied on the device under test, heated-up to 175°C while avoiding overheating of the auxiliary components. The main difference in this work compared to [7], is that the Fraunhofer-IZM [8-9] sensor allowing to measure the drain-source pulsed current of the DUT is not implemented. The drain source current in this setup is measured by using the current mirror connected to  $R_{SENSE}$  (Fig. 3).

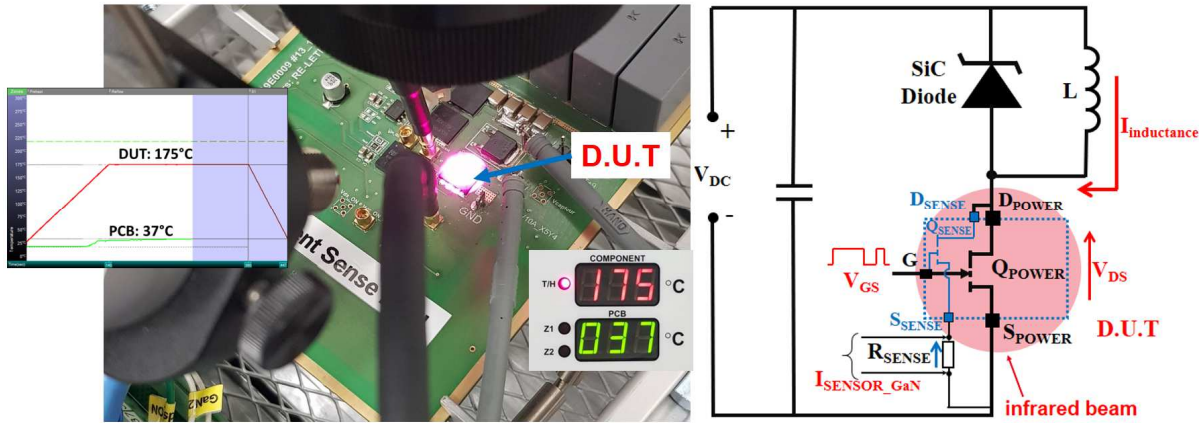


Fig. 3: High temperature set-up with a local heating-up on device under test by using an infrared beam

Fig. 4 shows the experimental results of the sensitivity of the integrated current mirror for three different temperatures (25°C, 125°C and 175°C). The integrated sensor responds with a sensitivity between 60mV/A and 45mV/A for a switched current between 3 A and 8 A. Due to the different temperature coefficients of the GaN HEMT device and  $R_{SENSE}$  with a very low temperature variation (10 ppm/°C) the sensitivities depend widely on the temperatures. As the observations under the infrared beam station, the device is auto-heat up when the characterized currents are applied; the higher the applied current is the higher of the ON-state resistance of DUT appears. In the next generations of this integrated current sensor,  $R_{SENSE}$  will be integrated inside the device to give a homogeneous behavior to the temperatures.

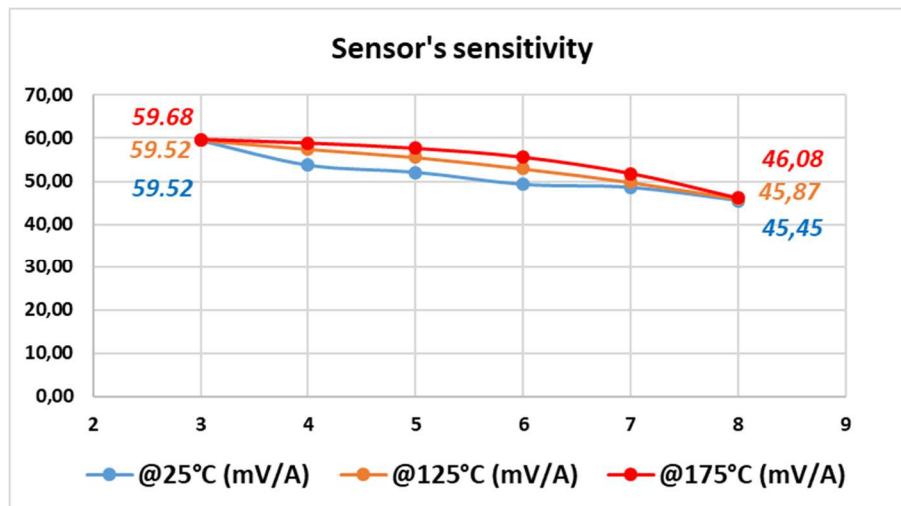


Fig. 4: High temperature characterizations of the sensor's sensitivity

Fig. 5 shows the main waveforms of an experiment in a typical DPT when DUT is heated up to 175°C. As mentioned in Fig. 3, the current on the inductance is on Chanel 1, the drain-source voltage  $V_{DS}$  is on Chanel 2, the control signal on the gate  $V_{GS}$  is on Chanel 3. With a pre-defined sensitivity, the

drain-source current of GaN power device is measured by the integrated sensor on Chanel 4, this current is extrapolated from the measured voltage on  $R_{SENSE}$ . In this experiment, the current in the inductance were configured at the value of 8A, the sensor's sensitivity is took at  $175^{\circ}\text{C}/8\text{A}$ .

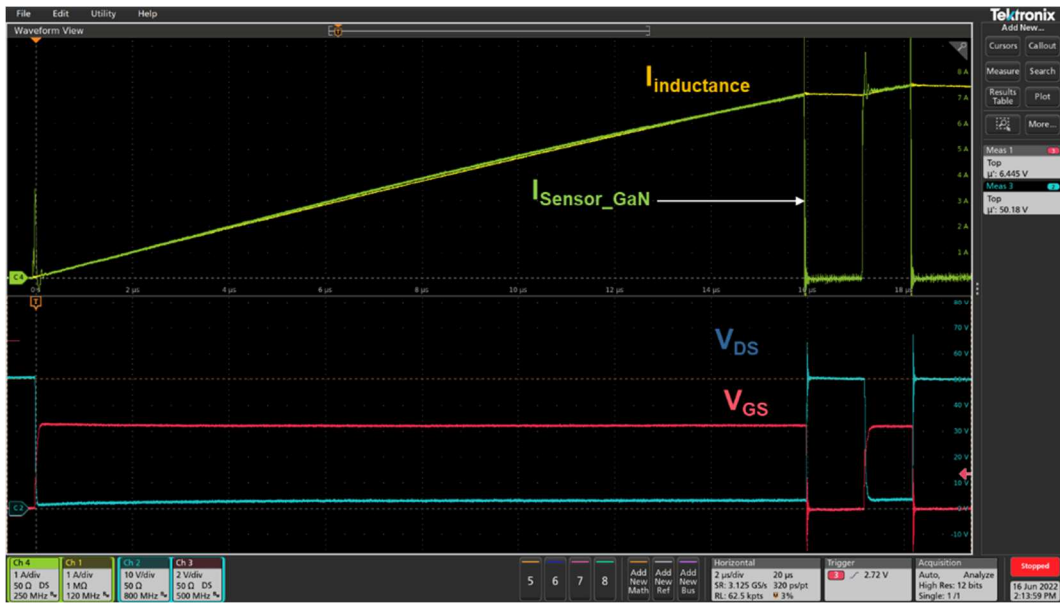


Fig. 5: Experimental waveforms of the DPT at  $175^{\circ}\text{C}$

Fig. 6 presents the DPT currents in power GaN device by its integrated sensor at six different temperatures from  $25^{\circ}\text{C}$  to  $175^{\circ}\text{C}$ , the current in the inductor (see Fig. 3) is measured separately by a commercial current probe (TCP0030A).

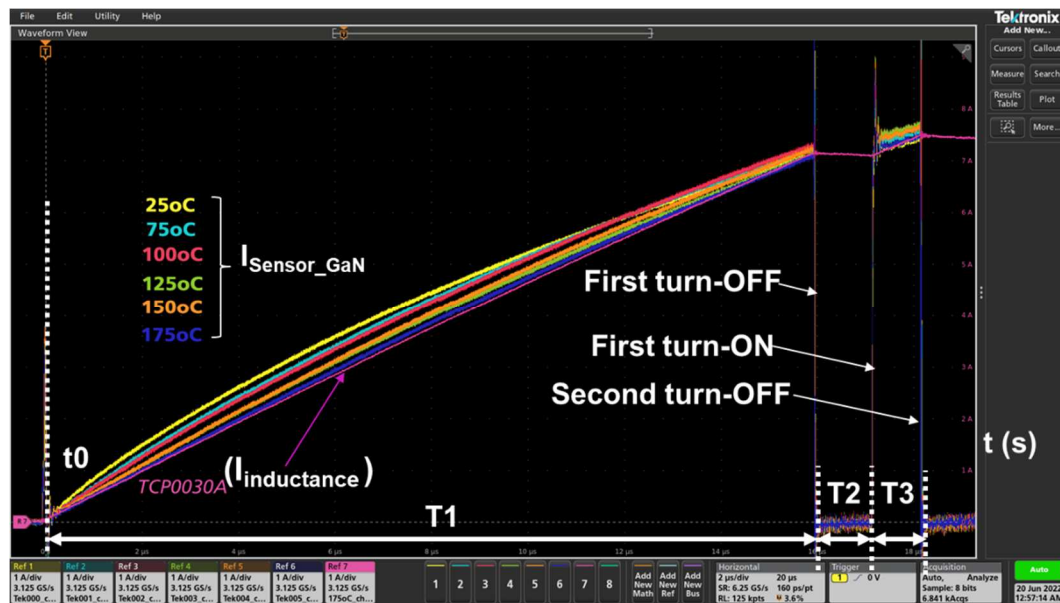


Fig. 6: Superimposed DPT currents by integrated sensor  $I_{SENSOR\_GaN}$  and inductor's current from  $25^{\circ}\text{C}$  to  $175^{\circ}\text{C}$

In this typical DPT, there are three interval T1, T2 and T3 in order to turn-ON and turn-OFF the DUT at a pre-configured current value. To reach the configured current for the first turn-OFF during T1, the current in inductance is charged by a constant input DC voltage ( $V_{DC}$  in Fig. 3); these first parts of all the measured currents are zoomed in Fig. 7. As we can see, the measure at  $175^{\circ}\text{C}$  is closest to the current by TCP0030A.

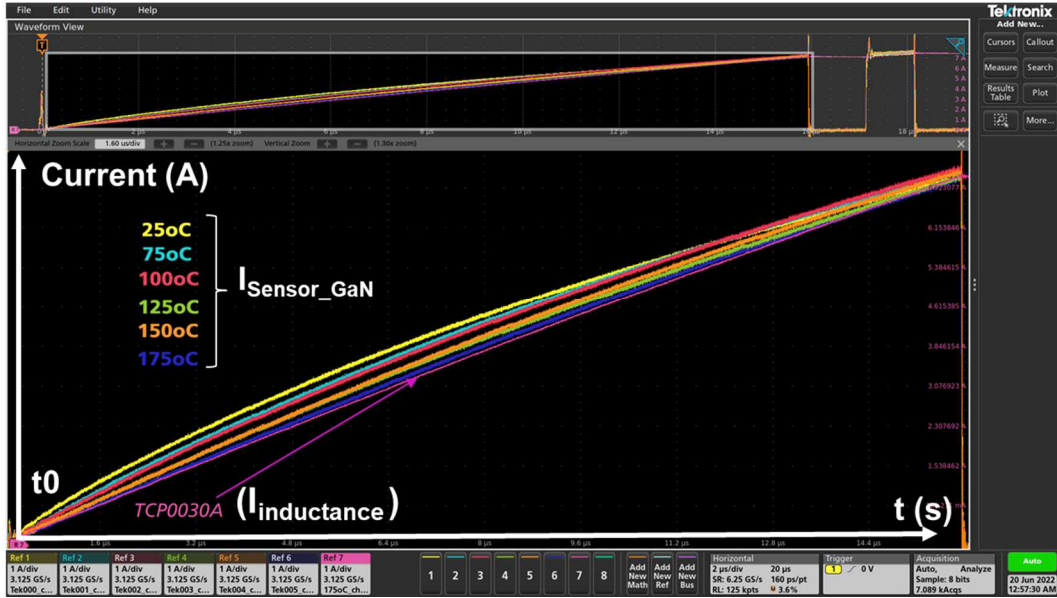


Fig. 7. Zoom in the first parts of measured currents before the first turn-OFF of DPT at different temperatures

The sensor measures this increasing portion of the current as a function of time. Thanks to these increasing curves between 0 A and 8A and at six temperatures, all the useful points characterize the response of the integrated current sensor in GaN device. Then the real transfer function ( $I_{sense}/I_{power}$ ) is presented theoretically in the previous section.

By replacing the  $R_{DS-ON}$  value of the current mirror by its proportion with respect to the power part, then the current transfer function is written as:

$$Gain_1 = \frac{I_{SENSE}}{I_{POWER}} \approx \frac{R_{DS-ONPOWER}}{50 \cdot R_{DS-ONPOWER} + R_{SENSE}} \approx 0.005$$

where  $R_{DS-ONPOWER}$  in the order of 80 mΩ at 25°C and  $R_{SENSE} = 10 \Omega$

This  $Gain_1$  represents the first stage of the integrated sensor in GaN power device without the unit because it is a ratio of currents. The second stage named  $Gain_2$  is represented by the  $R_{sense}$  that makes a current-voltage conversion (by shunt measurement) which produces a total gain of the sensor as follow

$$G_{SENSOR} = Gain_1 \times Gain_2 = 0.005 \times 10 V/A \approx 50 mV/A$$

This equation represents the total Gain of the complete sensor transfer function in Fig. 8.

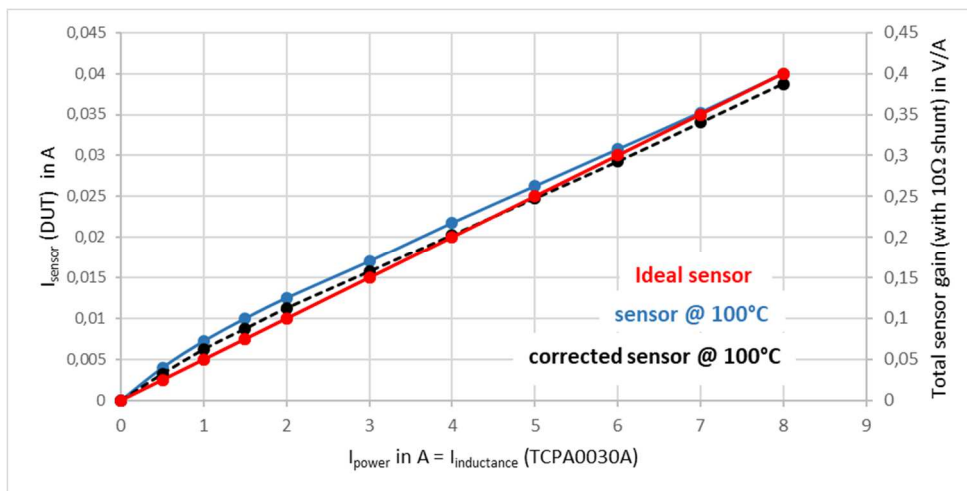


Fig. 8. Linearity of the sensor with  $Gain_1$  (left scale) and  $G_{SENSOR}$  (right scale) coefficients.

In this figure, a current probe (TCP0030A) with another corrected gain gives the dash line. For these measurements, a smallest error deviation at each point by adjusting precisely the gain of the oscilloscope probe (dash line) can be obtained.

In this way, the final measurement gain could be slightly corrected for the needs of the experiment by a third gain, so called Gain<sub>3</sub> with a value close to 1, the final gain of the sensor (dash line in Fig. 8) can be written as:

$$G_{SENSOR-FINAL} = Gain_1 \times Gain_2 \times Gain_3 = 0,005 \times 10 \text{ V/A} \times 0.99 = 49.5 \text{ mV/A}$$

Follow up the experimental results, the linearity of the current sensor is much better as the temperature increases, the tests at 150°C and 175°C giving the best results.

With this approach, the auto-heatup phenomena is slightly different between the sensor part behavior and the power part behavior on this die that explains the changes of the sensitivity of the sensor in function of the level of measured currents at a fixed temperature. However further studies must be undertaken in order to understand the evolution of self-heating as a function of current levels, and in particular if the improvement in linearity of the sensor at 150°C and 175°C comes from the fact that the contribution of self-heating decreases as the temperature levels increase.

In the next version of this integrated sensor, R<sub>SENSE</sub> should be integrated and the corrected coefficient must be given at different temperature and current values (by adding a small external electronic correction circuit for example) in order to get the most linear response possible at any configuration. Fig. 9 zooms in the first turn-ON and the second turn-OFF of the measured current at 8 A by the integrated sensor as the second pulse of the DPT, after the calibrations, these observed edges on the sense device share similar behaviors of the power device.

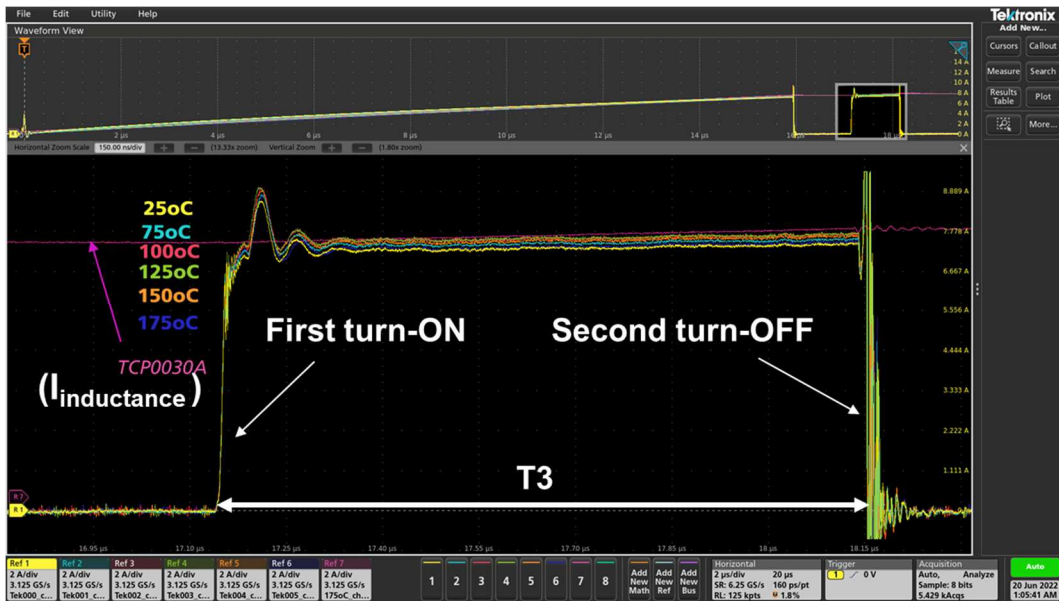


Fig. 9. The second pulse by the integrated sensor during the third interval T3

Fig. 10 and Fig. 11 show the rise times and fall time of the measured current by the integrated sensor at six different temperatures from 25°C to 175°C, the slew-rates of the current are 800 A/μs and 8200 A/μs for the rise time and fall time, respectively.

The rise times  $t_R$  of the current from 10% to 90% of the values are 8.045 ns at different temperature. The equivalent bandwidth of the current sensor for the solicitation at a positive step is therefore classically:

$$Bandwidth_{at-3dB} = \frac{0.35}{t_R} = \frac{0.35}{8.045 \text{ ns}} = 43.5 \text{ MHz}$$

The fall times  $t_F$  of the current from 90% to 10% of the values are shorter and the equivalent bandwidth of the sensor for the stress at a negative step varies between 308.7 MHz at 25°C and 274.1 MHz at 175°C.

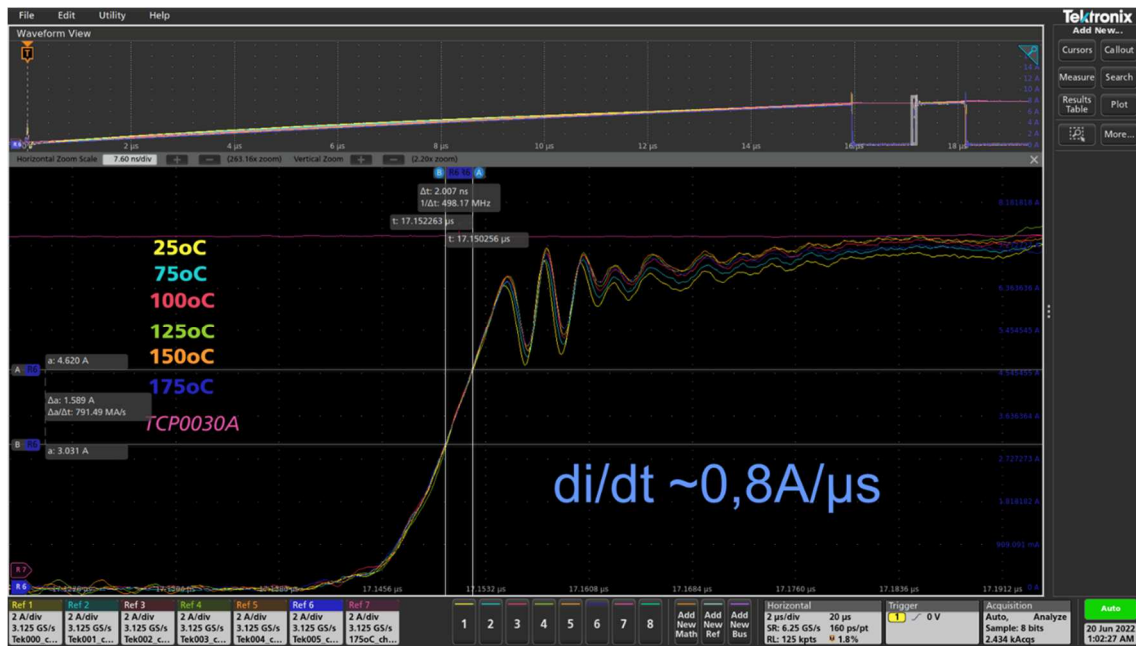


Fig. 10: Rise times of 8ns, the currents at 25°C, 75°C, 100°C, 125°C, 150°C and 175°C

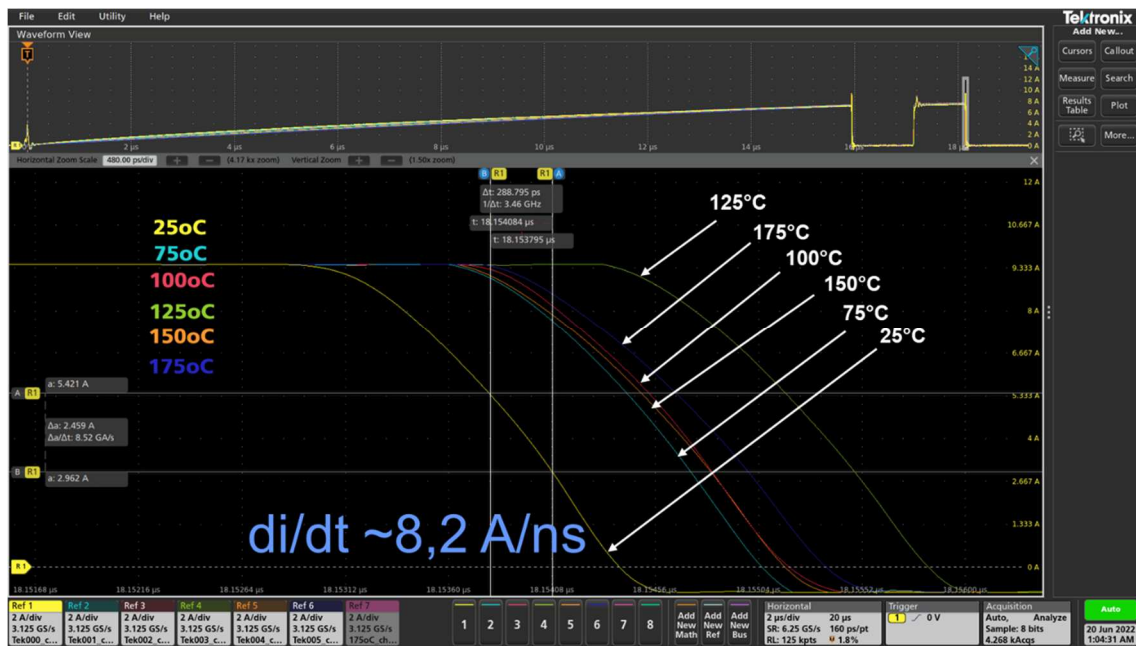


Fig. 11. Fall time of 1.2ns, the current at 25°C, 75°C, 100°C, 125°C, 150°C and 175°C

These fall times increase slightly at the higher temperatures and are represented in Fig. 12. The current-mirroring technique is implemented in this work, where the measured currents have the similar behavior of the current through GaN power transistor; we could expect the responses at these given values. It is nevertheless necessary to check that the entire measurement chain responds well to the sufficient bandwidth. For this, a shunt and a voltage probe with the bandwidth of 1GHz are used to extract the measured values of the integrated sensor; Fig. 12 shows these measured values on the red line are still in the measurable zone.

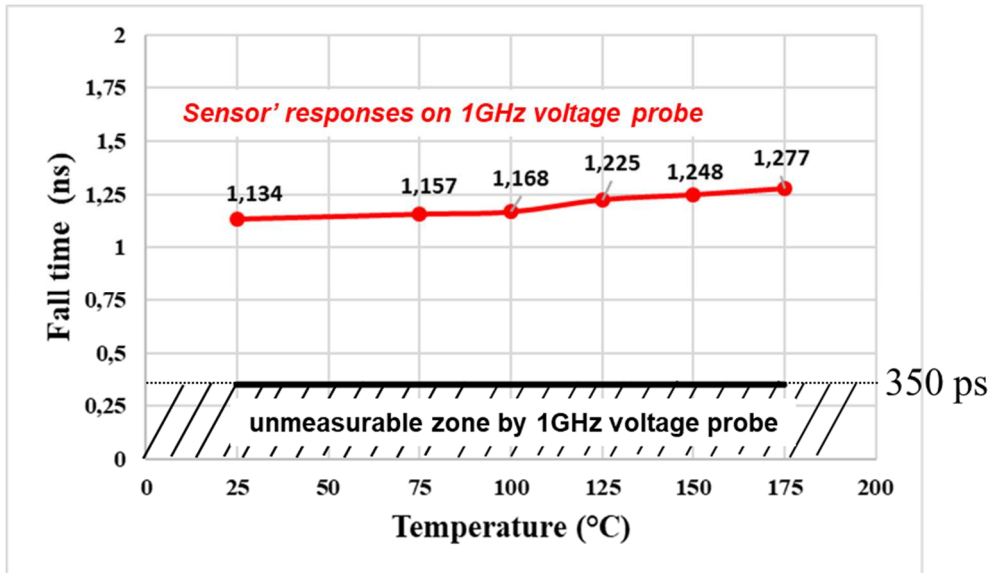


Fig. 12. Fall times at different temperatures from 25°C to 175°C (red line) and the unmeasurable zone

These experimental results show full functions of the integrated current sensor in a monolithic GaN HEMT device. By using this sensor, we can remove the high-speed current sensor that add the parasitic inductance in the power loop. The current-mirroring technique makes the behavior of the measured current similar to the current on the power devices.

In other hand, with a gate driver, this current sensor can use for protect very quickly the GaN device against the short-circuit in a specific application.

However, this integrated device show its limitation on the stability of the sensitivity with the temperature and the characterized value of the current. Authors are going to make a new version of this current sensor with integrated  $R_{SENSE}$ , in order to mitigate the dependent of the measures on the temperatures and the currents.

## Conclusion

This work presents a full-integrated current sensor inside a GaN power device. The current sensing approach is current mirroring, measuring a copy of the current in a smaller device with similar thermal behavior, making this approach very stable even in high temperature, up to 175°C. The details of the calibration circuit at different temperature and current were demonstrated. And the high temperature characterizations were given. This sensor need to be improved to have a linear response at any value of the temperature. In a dynamic characterization, this sensor could be used to measure the rising and falling edges of the current through the GaN power devices. Moreover, the integrated sensor could be implemented with a gate driver on a monolithic GaN device to protect the device against the short-circuit event within several nanosecond.

## References

- [1] Yole report on Power SiC 2020: Materials, Devices and Applications, Yole 2020
- [2] Yole report GaN power 2021: epitaxy, devices, applications and technology trends, Yole 2021
- [3] J. Wang, M. H. Hedayati, D. Liu, S-E. Adami, H. C. P. Dymond, J. O. Dalton, B. H. Stark “Infinity Sensor: Temperature Sensing in GaN Power Devices using Peak di/dt” 2018 IEEE Energy Conversion Congress and Exposition (ECCE), 2018
- [4] Z. Zhang, B. Guo, F. Wang, E. A. Jones, L. M. Tolbert, B. J. Blalock “Methodology for Wide Band-Gap Device Dynamic Characterization,” IEEE Trans. Power Electron., vol. 32, 2017
- [5] M. Biglarbegian, B. Parkhideh “Characterization of SenseGaN current-mirroring for power GaN with the virtual grounding in a boost converter” 2017 IEEE Energy Conversion Congress and Exposition (ECCE), 2017
- [6] S. Moench, R. Reiner, P. Waltereit, R. Quay, O. Ambacher, I. Kallfass “Integrated Current Sensing in GaN Power ICs” 2019 31st International Symposium on Power Semiconductor Devices and ICs (ISPSD), 2019
- [7] V. S. Nguyen, A. Bier, R. Escoffier, S. Catellani, J. Martin, C. Gillot “A high precision dynamic characterization bench with a current collapse measurement circuit for GaN HEMT operating at 175°C” PCIM Europe digital days 2021, May 2021
- [8] K. Klein, D. E. Hoene, and D. K.-D. Lang, “Comprehensive AC Performance Analysis of Ceramic Capacitors for DC link usage,” p. 7, 2017.
- [9] K. Klein, D. E. Hoene, and D. K.-D. Lang, “Power module design for utilizing of WBG switching performance,” p. 8, 2019